Euro. Jnl of Applied Mathematics (2011), *vol.* 22, *pp.* 187–216. © Cambridge University Press 2011
doi:10.1017/S0956792511000015

Instability thresholds in the microwave heating model with exponential non-linearity

ADAM ALCOLADO, THEODORE KOLOKOLNIKOV and DAVID IRON

Department of Mathematics and Statistics, Dalhousie University, Nova Scotia, Canada
email: adam.alcolado@dal.ca, tkolokol@gmail.com, iron@mathstat.dal.ca

(*Received 24 December 2009; revised 6 January 2011 and accepted 11 January 2011; first published online 8 February 2011*)

When ceramics are heated inside a microwave cavity, a well-known phenomenon is the occurrence of hot spots – localised regions of high temperature. This phenomenon was modelled by Kriegsmann ((1997), *IMA J. Appl. Math.* 59(2), pp. 123–146; (2001), *IMA J. Appl. Math.* 66(1), pp. 1–32) using a non-local evolution PDE. We investigate profile and the stability of hot spots in one and two dimensions by using Kriegsmann's model with exponential non-linearity. The linearised problem associated with hot-spot-type solutions possesses two classes of eigenvalues. The first type is the large eigenvalues associated with the stability of the hot-spot profile and in this particular model there cannot be instability associated with these eigenvalues. The second type is the small eigenvalues associated with translation invariance. We show that the hot spots can become unstable due to the presence of small eigenvalues, and we characterise the instability thresholds. In particular, we show that for the material with low heat conductivity (such as ceramics), and in the presence of a variable electric field, the hot spots are typically stable inside a plate (in two dimensions) but can become unstable for a slab (in one dimension) provided that the microwave power is sufficiently large. On the other hand, for materials with high heat conductivity, the interior hot spots are unstable and move to the boundary of the domain in either one or two dimensions. For materials with moderate heat conductivity, the stability of hot spots is determined by both the geometry and the electric field inside the microwave cavity.

Key words: Microwave heating; Bratu problem; Spike solutions

1 Introduction

The usage of microwave heating to join ceramic materials can result in the formation of stable and highly localised hot spots [16]. The formation of a localised hot spot cannot be explained using a simple linear theory. Several non-linear models of hot-spot formation have been proposed to explain this phenomenon (see, for example, review [5] and the references therein). In [1], a model for the temperature of a sample placed in a resonant chamber is derived. A wave guide keeps the amplitude of the microwaves constant along one axis. The formation of a stable hot spot is the result of considering a temperature-dependent electrical conductivity in conjunction with a local detuning in the resonant chamber containing the sample. The electrical conductivity changes occurring in the sample interfere with the formation of a standing wave in the resonant chamber. These considerations result in the following non-local reaction–diffusion

https://doi.org/10.1017/S0956792511000015 Published online by Cambridge University Press

equation

$$U_\tau = D\Delta U - 2\left(U + b[(U+1)^4 - 1]\right) + \frac{Pf(x)G(U)}{(1+\chi\int_\Omega f(x)G(U)\,dx)^2}, \quad x \in \Omega, \tag{1.1}$$

$$\partial_n U = 0, \quad x \in \partial\Omega. \tag{1.2}$$

Here, $f(x)$ is proportional to the square of the magnitude of the electric field along the sample, $G(u)$ is the scaled temperature-dependent electrical conductivity, D is the constant thermal diffusivity, $\chi > 0$ is a parameter based on the geometry of the sample and the Q-factor of the cavity (see [1]), $b \ll 1$ is the ratio of radiative to convective heat loss along the axis of the sample at the ambient temperature and $P > 0$ is the non-dimensional power of the resonant cavity mode. The form of $f(x)$ is determined by the wave guide used, as well as the geometry of the chamber and placement of the sample within the chamber. In [12], the sample is placed across the chamber and the wave guide keeps the electric field constant along the axis of a thin cylindrical sample. In this instance, the hot spot is actually unstable and propagates slowly exponentially along the sample until reaching the boundary of the domain [8]. In [13], a thin cylindrical sample is placed along the wave guide and the electric field may then vary along the length of the sample. Under certain additional assumptions on the parameters, it was shown in [8] that the hot spot will travel along the length of the sample until reaching a local maximum of f. The function $G(u)$ is the dimensionless electrical conductivity of the sample. We will consider a realistic exponential model $G(U) = e^{cU}$. We will also consider the small Biot number (b). For ceramics, the thermal diffusivity D is typically small. We make a further simplification by assuming that $\chi\int_\Omega f(x)e^{cU}\,dx \gg 1$. This assumption is consistent with most applications where the hot spot is observed [8]. In the non-dimensional form, we obtain

$$u_t = d^2\Delta u - u + \frac{pf(x)e^u}{(\int_\Omega f(x)e^u)^2}, \quad x \in \Omega; \quad \partial_n u = 0, \quad x \in \partial\Omega, \tag{1.3}$$

where $p = \frac{cP}{2\chi^2}$ and $d = \sqrt{\frac{c}{2}D}$. While the diffusivity coefficient d^2 is typically small for ceramic materials, we will also consider the more general mathematical problem, where d may be of $O(1)$. For example, in two dimensions and with $d = 1$, this model is related to the Liouville equation [15]. We will also consider the general form of $f(x)$, not restricted to the standard geometries and wave guides. Equation (1.3) is the starting point of our analysis.

Let us summarise the main results of this paper. We consider the equilibrium hot-spot solutions on a one-dimensional (1D) interval, a bounded 2D domain and a 2D disk. The hot-spot location and its stability is determined by the geometry of the problem as well as the electric field strength $f(x)$. The detailed results for one and two dimensions are given in Sections 2 and 3, respectively (Principal Results 2.1 and 2.2 for one dimension, and Principal Results 3.1 and 3.2 for two dimensions). In particular, the hot spots are found to exist provided that the power p is sufficiently large, even for relatively large value of the thermal diffusivity d. An important case is the radially symmetric domain and $f(x) = f(|x|)$, which we now describe. In this case, by symmetry, the hot spot is located at the centre of the domain. For a disk domain $\Omega = B_L(0) = \{x : |x| \leqslant L\} \subset \mathbb{R}^2$ and a radially symmetric electric field strength $f(x) = f(|x|)$, we find that the hot spot is stable

https://doi.org/10.1017/S0956792511000015 Published online by Cambridge University Press

with respect to both the large and small eigenvalues provided that

$$-\frac{f''(0)}{f(0)} \geqslant \frac{2}{d^2}\left(\frac{K_0''(L/d)}{I_0''(L/d)} - \frac{K_0'(L/d)}{I_0'(L/d)}\right), \tag{1.4}$$

where I_0 and K_0 are Bessel functions; it is unstable with respect to the small eigenvalues if the inequality in (1.4) is reversed. For typical ceramics with $d \ll 1$, the stability condition (1.4) reduces to

$$-\frac{f''(0)}{f(0)} \geqslant \frac{4\pi}{d^2} e^{-2L/d}. \tag{1.5}$$

Since the right-hand side of (1.5) is exponentially small, the 2D hot spot for a ceramic material will be stable at the centre provided that f has a maximum value at the centre.

For a 1D situation with $f(x) = f(-x)$ and $\Omega = [-L, L]$, we show in Principal Result 2.2 that the hot spot is stable provided that

$$L/d \gg 1 \qquad \text{and} \qquad -\frac{f''(0)}{f(0)} \geqslant \frac{4}{d^2} \ln\left(\frac{p}{2d^2 f(0)}\right) \exp\left(\frac{-2L}{d}\right); \qquad \Omega = [-L, L] \in \mathbb{R}. \tag{1.6}$$

Both of these requirements are necessary; if one of them does not hold, then the hot spot was found to be unstable. In particular, this shows that in one dimension, the heat diffisivity d must be small. In addition, the hot spot can be distabilised if the power p is sufficiently large. This is unlike the 2D case, where the stability result is independent of the power p. Equations (1.4) and (1.6) also show that in either one or two dimensions, the hot spot cannot be stable if $f(x)$ is constant; a necessary condition for the radially symmetric case is that $f(x)$ must have a maximum at the origin.

In Section 5, we study numerically and analytically how the formation of the hot spots depends on the power p. For the case of small diffusion $d \ll 1$, we show that the necessary condition for hot-spot formation is that $p > p_c$, where p_c is the critical power given by

$$p_c = Me\left(\int_\Omega W\left(-\frac{f(x)}{Me}\right) dx\right)^2, \tag{1.7}$$

where $M = \max_{x\in\Omega} |f(x)|$ and $W(x)$ is the principle branch of the Lambert W function (which satisfies $x = W(x)e^{W(x)}$ with $-1 < W(x)$). Finally, we study the possibility of a pattern with two spots. We show in Section 5 that two hot spots cannot be stable. Moreover, the unstable mode corresponds to a competition instability, whereby one of the two spots is rapidly absorbed by the other. This is analogous to the so-called shadow limit of reaction–diffusion equations, see for example [7, 9], where a similar phenomenon is observed for the Geirer–Meinhardt model. We conclude with some discussion of open problems in Section 6.

We note that the results in this paper rely on the use of careful but formal asymptotics. No attempt has been made to provide a rigorous justification. However, careful numerics were used to verify all of the results.

https://doi.org/10.1017/S0956792511000015 Published online by Cambridge University Press

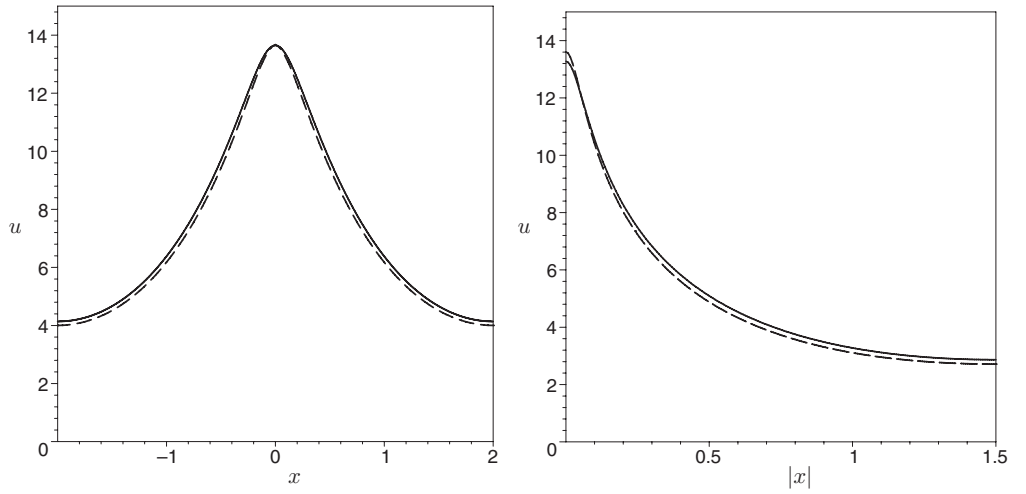

FIGURE 1. (a) Stationary hot-spot solution to (2.1) in one dimension. The parameters are $f(x) = 1$, $L = 2$, $d = 1$ with $p = 1.144 \times 10^9$ chosen so that (2.2) yields $\alpha = 0.0001$. Solid curve represents the numerical solution to the boundary value problem (2.1). Dashed curve is the uniform asymptotic approximation (2.8). (b) Hot-spot solution to (3.1) in two dimensions on a disk of radius $L = 1.5$. Other parameters are $f(x) = 1$, $d = 1$ with $p = 1.7217 \times 10^5$ chosen so that (3.2) yields $\alpha = 0.004$. Solid curve represents the numerical solution to the boundary value problem (3.1). Dashed curve is the uniform asymptotic approximation (3.51).

2 One dimension

In this section, we study hot spots on a 1D domain $\Omega = [-L, L]$. We first construct a stationary hot-spot solution using matched asymptotics. An example of such a hot spot is shown in Figure 1(a).

The steady state problem is

$$u_{xx} - \frac{1}{d^2}u + \alpha f(x)e^u = 0, \quad u_x(\pm L) = 0, \quad \text{where} \tag{2.1}$$

$$\alpha := \frac{p}{\left(d\int_{-L}^{L} f(x)e^u\,dx\right)^2}. \tag{2.2}$$

Roughly speaking, the hot-spot solution consists of an inner region of hot temperature, where the exponential term in (2.1) is dominant, and of an outer layer of colder temperature, where the background effects dominate. The location x_0 of the stationary hot spot is determined by both the electric field strength $f(x)$ and the boundary effects. We summarise the construction as follows.

Principal Result 2.1 *Suppose that either $p \gg 1$ or $d \ll 1$, with all other parameters of $O(1)$. Then, (2.1) and (2.2) admit a hot-spot solution concentrated at the location x_0, given asymptotically by*

$$\frac{\sinh\left(\frac{2x_0}{d}\right)}{\sinh\left(\frac{2L}{d}\right)} + \mu\frac{f'(x_0)}{f(x_0)} \sim 0, \tag{2.3}$$

https://doi.org/10.1017/S0956792511000015 Published online by Cambridge University Press

where $\mu \ll 1$ is the spatial extent of the hot spot centred at x_0, asymptotically given by

$$\mu \sim \frac{d}{\ln\left(\frac{p}{2d^2 f(x_0)}\right)}\left(\frac{\cosh\left(\frac{2x_0}{d}\right)}{\sinh\left(\frac{2L}{d}\right)} + \coth\frac{2L}{d}\right). \tag{2.4}$$

Inside the hot spot, the temperature profile has the shape

$$u(x) \sim \ln\left\{\frac{p}{2\alpha\mu^2 f(x_0)}\operatorname{sech}^2\left(\frac{x}{2\mu}\right)\right\}, \quad |x - x_0| \ll \mu, \tag{2.5}$$

where α, as defined in (2.2), is asymptotically given by

$$\alpha \sim \frac{d^2 4}{p\mu^2}. \tag{2.6}$$

Away from the hot spot, the temperature profile is

$$u(x) \sim \frac{2}{\mu}G(x, x_0), \quad |x - x_0| \gg \mu, \tag{2.7}$$

where $G(x, x_0)$ is Green's function defined in (2.18).

By combining (2.5) and (2.7), for the case of a symmetric hot spot ($x_0 = 0$, $f(x)$ is even), a composite solution that is uniformly valid on $[-L, L]$ is given by

$$u(x) \sim \ln\left\{\frac{1}{4}\operatorname{sech}^2\left(\frac{x}{2\mu}\right)\right\} + |x|/\mu + \frac{\ln\left(\frac{2}{\mu^2 f(x_0)\alpha}\right)}{\cosh(L/d)}\cos\left(\frac{|x| - L}{d}\right). \tag{2.8}$$

Figure 1(a) shows a favourable comparison between the composite asymptotic solution and the numerical solution to the full problem (2.1). In Figure 2(a), the effect of variation of the magnitude of the electric field strength, $f(x)$ along the length of the sample, on the hot-spot location is shown. Again, a favourable comparison between full numerics and the asymptotic formula for x_0 (2.3) is observed.

Next, we address the stability of the hot spot with respect to time. By linearising near the steady state

$$u(x, t) = u(x) + e^{\lambda t}\phi(x), \quad \phi \ll 1,$$

we are led to the study of the following eigenvalue problem:

$$\frac{\lambda}{d^2}\phi = \phi_{xx} - \frac{1}{d^2}\phi + \alpha f(x)e^u\phi - 2\alpha^{3/2}p^{-1/2}d^{-1}f(x)e^u\int_{-L}^{L} f(x)e^u\phi dx. \tag{2.9}$$

Note that (2.9) is self-adjoint; as a consequence, all of its eigenvalues are purely real. The problem (2.9) admits large eigenvalues of $O(\frac{1}{\mu^2})$ as well as eigenvalues that arise due to the translation invariance of the inner solution, which we will call small eigenvalues. The large eigenvalues are studied in Section 4, where it is shown that they are all negative. Thus, the stability is controlled by the sign of the small eigenvalues. We summarise our findings below.

https://doi.org/10.1017/S0956792511000015 Published online by Cambridge University Press

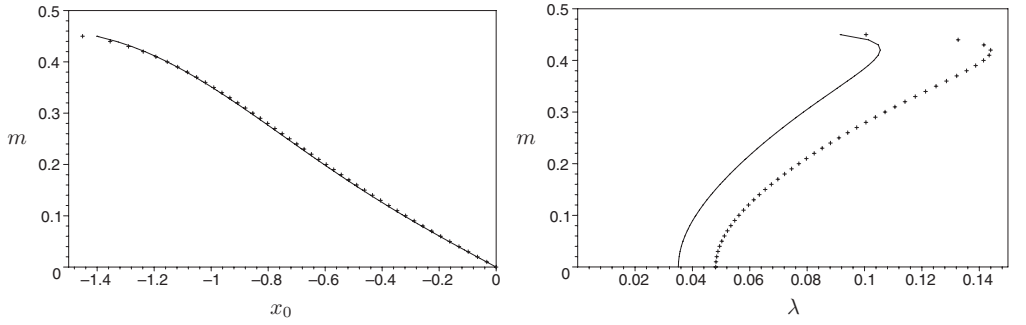

FIGURE 2. (a) The plot of hot-spot centre x_0 versus m, with $f(x) = 1 + mx$, $L = 2.7$, $d = 1$, $\alpha = 3.16 \times 10^{-5}$. Crosses denote the numerical solution of (2.1). Solid line denotes the asymptotic prediction given by (2.3) with μ given by (2.23). (b) The plot of x_0 versus λ, where λ is the eigenvalue with largest real part, in this case the small eigenvalues. Crosses denote the values of λ as numerically computed from (2.9). Solid line denotes the asymptotic prediction given by (2.42).

Principal Result 2.2 *Consider a hot-spot solution as constructed in Principal result 2.1. In the limit* $\mu \to 0$, *there are two cases.*

(1) $d/L = O(1)$: *The hot spot is unstable.*

(2) $d/L \ll 1$: *The hot spot is stable if and only if* $\lambda < 0$, *where* λ *is given by*

$$\lambda \sim 2\mu d \left(\frac{f''(x_0)}{f(x_0)} - \left(\frac{f'(x_0)}{f(x_0)} \right)^2 \right) + 8 \exp\left(\frac{-2L}{d} \right) \cosh\left(\frac{x_0}{d} \right), \qquad d/L \ll 1. \tag{2.10}$$

In the first case, the unstable eigenvalue λ *is given implicitly by (2.42).*

Formula (2.10) is an asymptotic estimate to the small eigenvalue of (2.9). Figure 2(b) shows that the asymptotic formula (2.10) is in good agreement with the numerically computed solution to the eigenvalue problem (2.9). For a radially symmetric case where $f(x) = f(|x|)$ and $x_0 = 0$, the stability criterion of Principal Result 2.2 in conjunction with (2.2) yields the formula (1.6).

Derivation of Principal Result 2.1 The derivation consists of two steps. We first determine the leading-order profile and the spatial extent μ of the hot spot. In the second step, the location x_0 of the hot spot is determined at the next order of the expansion.

Step 1. Hot-spot profile In order to determine the temperature profile and the spatial extent of the hot spot, we expand near its centre $x = x_0$ as

$$x = x_0 + \mu y; \tag{2.11a}$$

$$f(x) = f_0 + \mu y f_0' + \cdots \qquad \text{where } f_0 \equiv f(x_0),\ f_0' \equiv f'(x_0); \tag{2.11b}$$

$$u(x) = U(y) = U_0(y) + \mu U_1(y) + \cdots, \tag{2.11c}$$

where $\mu \ll 1$ is the spatial extent of the hot spot, to be determined later. Equation (2.1)

https://doi.org/10.1017/S0956792511000015 Published online by Cambridge University Press

then becomes

$$U_{yy} + \frac{\mu^2}{d^2} U + \mu^2 \alpha f(x_0 + \mu y) e^U = 0.$$

Next, we change variables

$$U(y) = \ln \left\{ \frac{V(y)}{\alpha \mu^2 f(x_0 + \mu y)} \right\} \tag{2.12}$$

and expand

$$V = V_0 + \mu V_1 + \cdots,$$
$$U = U_0 + \mu U_1 + \cdots.$$

The equation for V_0 is then

$$V_{0yy} - \frac{V_{0y}^2}{V_0} + V_0^2 = 0. \tag{2.13}$$

An explicit solution is given by

$$V_0 = \frac{1}{2} \operatorname{sech}^2 \left(\frac{y}{2} \right). \tag{2.14}$$

Note that (2.13) admits a scaling invariance $V_0 = a^{-2} \hat{V}_0$; $y = a\hat{y}$. However, we can set $a = 1$ by an appropriate re-labelling of μ.

Next, we consider the outer region of (2.1). We estimate

$$u_{xx} - \frac{1}{d^2} u = -C_0 \delta(x - x_0), \tag{2.15}$$

where $\delta(x - x_0)$ is the Dirac delta function with support at x_0 and the constant C_0 is given by

$$C_0 = \int_{-L}^{L} \alpha f(x) e^u dx \sim \frac{1}{\mu} \int_{-\infty}^{\infty} V_0(y) dy \sim \frac{2}{\mu}. \tag{2.16}$$

The solution to (2.15) is therefore

$$u \sim \frac{2}{\mu} G(x, x_0), \tag{2.17}$$

where G is Green's function satisfying

$$G_{xx} - \frac{1}{d^2} G = -\delta(x - x_0); \quad G_x(\pm L, x_0) = 0$$

and is explicitly given by

$$G(x, x_0) = \frac{d}{\sinh\left(\frac{2L}{d}\right)} \begin{cases} \cosh\left(\dfrac{x - L}{d}\right) \cosh\left(\dfrac{x_0 + L}{d}\right), & x > x_0, \\ \cosh\left(\dfrac{x_0 - L}{d}\right) \cosh\left(\dfrac{x + L}{d}\right), & x < x_0. \end{cases} \tag{2.18}$$

The spatial extent of the hot spot μ is now determined by matching the inner and outer

https://doi.org/10.1017/S0956792511000015 Published online by Cambridge University Press

solution. In order to do so, we write the inner solution in the outer variables as $|y| \to \infty$. Note that

$$V_0 \sim 2\exp(-|y|), \quad |y| \to \infty$$

so that from (2.12) we get

$$U_0 \sim \ln\left(\frac{2}{\alpha\mu^2 f_0}\right) - |y|, \qquad |y| \to \infty, \tag{2.19}$$

$$\mu U_0 \sim \mu \ln\left(\frac{2}{\alpha\mu^2 f_0}\right), \qquad \mu \ll |x - x_0| \ll 1. \tag{2.20}$$

On the other hand, we expand G in Taylor series around $x = x_0$. We write

$$G(x, x_0) \sim G_0 + (x - x_0)\, G'_{0^+}, \quad 0 < x - x_0 \ll 1,$$
$$G(x, x_0) \sim G_0 + (x - x_0)\, G'_{0^-}, \quad 0 < x_0 - x \ll 1,$$

where

$$G_0 = G(x_0, x_0) = \frac{d}{2}\left(\frac{\cosh\left(\frac{2x_0}{d}\right)}{\sinh\left(\frac{2L}{d}\right)} + \coth\frac{2L}{d}\right), \tag{2.21}$$

$$G'_{0^\pm} = \frac{\partial}{\partial x} G(x, x_0)\bigg|_{x=x_0^\pm} = \frac{1}{2}\left(\frac{\sinh\left(\frac{2x_0}{d}\right)}{\sinh\left(\frac{2L}{d}\right)} \pm 1\right). \tag{2.22}$$

Substituting (2.21) and (2.20) into (2.17) we obtain an equation for μ,

$$\mu \ln\left(\frac{2}{\alpha\mu^2 f_0}\right) = d\left(\frac{\cosh\left(\frac{2x_0}{d}\right)}{\sinh\left(\frac{2L}{d}\right)} + \coth\frac{2L}{d}\right). \tag{2.23}$$

It remains to verify the consistency condition $\mu \ll 1$. We evaluate

$$\int_{-L}^{L} f e^u \, dx \sim \int_{-\infty}^{\infty} \frac{V}{\alpha\mu^2} dy \sim \frac{2}{\alpha\mu}$$

so that

$$\frac{1}{\alpha\mu^2} \sim \frac{p}{d^2 4}, \tag{2.24}$$

$$\mu \sim \frac{d}{\ln\left(\frac{p}{2d^2 f_0}\right)}\left(\frac{\cosh\left(\frac{2x_0}{d}\right)}{\sinh\left(\frac{2L}{d}\right)} + \coth\frac{2L}{d}\right) \sim O\left(\frac{d}{\ln(p/d^2)}\right).$$

In particular, this equation is consistent provided that either $p \gg 1$ or $d \ll 1$ (with other parameters being $O(1)$).

Step 2. Hot-spot location The equation for the location x_0 is determined at a higher order. We have

$$U_0 + \mu U_1 = \ln\left\{\frac{V_0}{\alpha\mu^2 f_0}\frac{1 + \mu\frac{V_1}{V_0}}{1 + \mu\frac{y f'_0}{f_0}}\right\} = \ln\frac{V_0}{\alpha\mu^2 f_0} + \mu\left(\frac{V_1}{V_0} - y\frac{f'_0}{f_0}\right) \tag{2.25}$$

https://doi.org/10.1017/S0956792511000015 Published online by Cambridge University Press

so that

$$V_0 = \mu^2 \alpha f_0 e^{U_0}\big|_{-\infty}^{\infty}; \qquad V_1 = \left(U_1 + y\frac{f_0'}{f_0}\right) V_0, \tag{2.26}$$

and the first two orders in the inner variables are

$$U_{0yy} + V_0 = 0, \tag{2.27}$$

$$U_{1yy} + V_0 U_1 + V_0 y \frac{f_0'}{f_0} = 0. \tag{2.28}$$

Multiply (2.28) by U_{0y} and integrate from $-\infty$ to $+\infty$. Integrating by parts we obtain

$$\int_{-\infty}^{\infty} U_1(U_{0yyy} + V_0 U_{0y})dy + \frac{f_0'}{f_0}\int_{-\infty}^{\infty} y V_0 U_{0y} dy + (U_{1y}U_{0y} - U_1 U_{0yy})|_{-\infty}^{\infty} = 0. \tag{2.29}$$

Note that

$$V_{0y} = V_0 U_{0y}; \quad U_{0yy} + V_{0y} = 0$$

so that

$$\int_{-\infty}^{\infty} U_1 \left(U_{0yyy} + V_0 U_{0y}\right) dy = 0; \quad \text{and} \quad \int_{-\infty}^{\infty} y V_0 U_{0y} dy = -\int_{-\infty}^{\infty} V_0 = -2. \tag{2.30}$$

In order to evaluate the boundary term, first note that for large y we have

$$U_{0y} \to \mp 1, \qquad U_{0yy} \to 0 \qquad \text{as } y \to \pm\infty.$$

The behaviour of U_1 for large y is determined by matching to the outer solution. Recall that

$$U_0(y) + \mu U_1(y) \sim \frac{2}{\mu} G(x, x_0), \qquad x \to x_0, |y| \to \infty.$$

Writing the right-hand side in terms of inner variables, we have

$$G(x, x_0) = G(x_0 + \varepsilon y, x_0) \sim G_0 + y\mu G_{0\pm}', \quad y \gtrless 0,$$

where G_0 and $G_{0\pm}'$ are given by (2.21) and (2.22). For large $|y|$, we then obtain

$$\mu U_1 + y \sim 2y G_{0^+}', \quad y \gg 1,$$
$$\mu U_1 - y \sim 2y G_{0^-}', \quad y \ll 1,$$

so that

$$U_{1y}|_{y=\pm\infty} = \frac{1}{\mu}(2G_{0\pm}' \mp 1), \tag{2.31}$$

and finally,

$$\begin{aligned}(U_{1y}U_{0y} - U_1 U_{0yy})_{-\infty}^{\infty} &= -\frac{2}{\mu}(G_{0^+}' + G_{0^-}') \\ &= -\frac{2}{\mu}\frac{\sinh\left(\frac{2x_0}{d}\right)}{\sinh\left(\frac{2L}{d}\right)}.\end{aligned} \tag{2.32}$$

https://doi.org/10.1017/S0956792511000015 Published online by Cambridge University Press

Substituting (2.30) and (2.31) into (2.29) yields the equation for spike location,

$$\frac{\sinh\left(\frac{2x_0}{d}\right)}{\sinh\left(\frac{2L}{d}\right)} = -\mu\frac{f_0'}{f_0}. \tag{2.33}$$

This concludes the derivation of Principal Result 2.1. □

Derivation of Principal Result 2.2 We now turn to the stability of the hot spot. In the inner region $y = (x - x_0)/\mu$, we expand the eigenfunction as

$$\phi(x) = \Phi_0(y) + \mu\Phi_1(y) + \cdots. \tag{2.34}$$

Substituting (2.34), (2.11) and (2.13) into (2.9) we get at the leading order

$$\Lambda\Phi_0 = \Phi_{0yy} + V_0\Phi_0 - V_0\int_{-\infty}^{\infty} V_0\Phi_0\, dy, \tag{2.35}$$

where $\Lambda = \mu^2/d^2\lambda$; and V_0 is given in (2.13). Note that the spectrum of (2.35) admits a zero eigenvalue $\Lambda = 0$, $\Phi_0 = V_{0y}/V_0$, which corresponds to translation invariance. It will be shown in Principal Result 4.1 that all non-zero eigenvalues of (2.35) are negative. In view of this, we need to be only concerned with the zero translational eigenvalue. Since it is zero at leading order, its stability is determined by considering the correction terms that arise due to the outer region of (2.9) and the spatially inhomogeneous term $f(x)$. In the inner region, we estimate the eigenfunction by

$$\phi \sim u_x \sim \frac{V_x}{V}. \tag{2.36}$$

The integral term then becomes

$$\int_{-L}^{L} f e^u \phi dx \sim \int_{-\infty}^{\infty} \frac{V}{\alpha\mu^2}\left(\frac{V_y}{V}\right) dy = 0.$$

In order to obtain a solvability condition, multiply (2.9) by u_x and integrate. Upon integrating by parts we obtain

$$\frac{\lambda}{d^2}\int_{-L}^{L} \phi u_x\, dx = -u_{xx}\phi|_{-L}^{L} - \int_{-L}^{L} \alpha f' e^u \phi\, dx.$$

In the outer region for u and ϕ we have

$$\frac{\lambda}{d^2}\phi \sim \phi_{xx} - \frac{1}{d^2}\phi, \quad x \neq x_0,$$
$$0 \sim u_{xxx} - \frac{1}{d^2}u_x, \quad x \neq x_0.$$

https://doi.org/10.1017/S0956792511000015 Published online by Cambridge University Press

Let $D = [-L, L]\backslash\{x_0\}$. We have

$$\int_D \left(\phi_{xx} - \frac{1}{d^2}\phi - \frac{\lambda}{d^2}\phi\right) u_x dx \sim (u_x\phi_x - u_{xx}\phi)|_{-L}^{x_0^-} + (u_x\phi_x - u_{xx}\phi)|_{x_0^+}^{L} - \int_{-L}^{L} \frac{\lambda}{d^2}\phi u_x dx$$
$$\sim -u_{xx}\phi|_{-L}^{L} - \int_{-L}^{L} \frac{\lambda}{d^2}\phi u_x dx - (u_x\phi_x - u_{xx}\phi)|_{x_0^+}^{x_0^-} = 0.$$

Therefore, we obtain

$$-(u_x\phi_x - u_{xx}\phi)\,|_{x_0^-}^{x_0^+} \sim -\int_{-L}^{L} \alpha f' e^u \phi\, dx. \tag{2.37}$$

Now in the outer region we have $u \sim C_0 G(x, x_0)$. Let G^λ, N^λ be Green's functions satisfying

$$G^\lambda_{xx} - \frac{(1+\lambda)}{d^2} G^\lambda = -\delta(x - x_0), \quad G^\lambda_x(\pm L) = 0, \tag{2.38}$$

$$N^\lambda_{xx} - \frac{(1+\lambda)}{d^2} N^\lambda = -\delta'(x - x_0), \quad N^\lambda_x(\pm L) = 0. \tag{2.39}$$

By differentiating (2.38) with respect to x_0, we obtain

$$N^\lambda = -\frac{\partial G^\lambda}{\partial x_0}. \tag{2.40}$$

Explicitly, we have

$$G^\lambda(x, x_0) = \frac{1}{\omega \sinh(2L\omega)} \begin{cases} \cosh((x-L)\omega)\cosh((x_0+L)\omega), & x > x_0, \\ \cosh((x_0-L)\omega)\cosh((x+L)\omega), & x < x_0. \end{cases}$$

$$N^\lambda(x, x_0) = \frac{-1}{\sinh(2L\omega)} \begin{cases} \cosh((x-L)\omega)\sinh((x_0+L)\omega), & x > x_0, \\ \sinh((x_0-L)\omega)\cosh((x+L)\omega), & x < x_0, \end{cases}$$

where $\omega = \dfrac{\sqrt{1+\lambda}}{d}$.

Matching the inner and outer regions, we have $\phi \sim u_x \sim C_0 G_x$, where C_0 is given by (2.16). Thus, ϕ has a jump discontinuity $\phi|_{x=x_0^-}^{x=x_0^+} \sim -C_0$. On the other hand, N^λ has a jump discontinuity of -1 at x_0, $N^\lambda|_{x=x_0^-}^{x=x_0^+} = -1$. Therefore, in the outer region we get $\phi \sim C_0 N^\lambda(x, x_0)$. We then obtain

$$(u_x\phi_x - u_{xx}\phi)_{x_0^-}^{x_0^+} \sim -C_0^2 \left(G_x N^\lambda_x|_{x^-}^{x^+} - \frac{1}{d^2} G N^\lambda|_{x^-}^{x^+}\right). \tag{2.41}$$

Now N^λ_x is continuous at x_0, whereas G_x has a jump discontinuity of -1. Using (2.40), we then simplify

$$G_x N^\lambda_x|_{x^-}^{x^+} = -N^\lambda_x|_{x=x_0} = G^\lambda_{x_0 x}|_{x=x_0},$$

and similarly,

$$G N^\lambda|_{x^-}^{x^+} = -G|_{x=x_0}.$$

https://doi.org/10.1017/S0956792511000015 Published online by Cambridge University Press

Therefore,

$$(u_x\phi_x - u_{xx}\phi)_{x_0^-}^{x_0^+} \sim -C_0^2\left(G^{\lambda}_{x_0x}|_{x=x_0} + \frac{1}{d^2}G|_{x=x_0}\right).$$

$$\begin{aligned} G^{\lambda}_{x_0x}|_{x=x_0} &= \frac{\omega\sinh((x_0-L)\omega)\sinh((x_0+L)\omega)}{\sinh(2L\omega)} \\ &= \frac{\omega(\cosh(2x_0\omega)-\cosh(2L\omega))}{2\sinh(2L\omega)}, \quad \omega = \frac{\sqrt{1+\lambda}}{d}; \\ G|_{x=x_0} &= \frac{(\cosh(2x_0\omega_0)+\cosh(2L\omega_0))}{2\omega_0\sinh(2L\omega_0)}, \quad \omega_0 = \frac{1}{d} \end{aligned}$$

so that

$$(u_x\phi_x - u_{xx}\phi)_{x_0^-}^{x_0^+} = \frac{-4}{\mu^2}\left(\frac{\omega(\cosh(2x_0\omega)-\cosh(2L\omega))}{2\sinh(2L\omega)} + \frac{\omega_0(\cosh(2x_0\omega_0)+\cosh(2L\omega_0))}{2\sinh(2L\omega_0)}\right).$$

Next, we evaluate the right-hand side of (2.37). Using (2.36) and (2.12), we obtain

$$\begin{aligned} \int_{-L}^{L}\alpha f' e^u\phi\,dx &\sim \frac{1}{\mu^2}\int_{-L}^{L}\frac{f'}{f}V_x\,dx \sim \frac{-1}{\mu^2}\int_{-L}^{L}\left(\frac{f'}{f}\right)_x V\,dx \\ &\sim -\frac{1}{\mu}\left(\frac{f_0''}{f_0} - \frac{f_0'^2}{f_0^2}\right)\int_{-\infty}^{\infty}V_0\,dy \\ &\sim -\frac{2}{\mu}\left(\frac{f_0''}{f_0} - \frac{f_0'^2}{f_0^2}\right). \end{aligned}$$

The full equation for the eigenvalue is therefore

$$\frac{\omega(\cosh(2x_0\omega)-\cosh(2L\omega))}{\sinh(2L\omega)} + \frac{\omega_0(\cosh(2x_0\omega_0)+\cosh(2L\omega_0))}{\sinh(2L\omega_0)} \sim -\mu\left(\frac{f_0''}{f_0} - \frac{f_0'^2}{f_0^2}\right), \tag{2.42}$$

where

$$\omega = \frac{\sqrt{1+\lambda}}{d}, \quad \omega_0 = \frac{1}{d}.$$

From (2.33), it is clear that either $d/L \ll 1$ or else $x_0 \sim 0$. In the latter case we get

$$-\sqrt{1+\lambda}\tanh\left(L\frac{\sqrt{1+\lambda}}{d}\right) + \coth\left(\frac{L}{d}\right) \sim 0. \tag{2.43}$$

Now, note that the left-hand side is positive when $\lambda = 0$ and goes to $-\infty$ as $\lambda \to \infty$. Therefore (2.43) has a positive solution $\lambda > 0$. This shows the instability for case 1 of Principal Result 2.2. For the former case, we must have $\frac{L}{d} \ll 1$; $\omega \sim \omega_0$ so that $\lambda \ll 1$. We then expand in λ to obtain (2.10). This concludes the derivation. □

3 Two dimensions

The analysis in two dimensions is along the lines of the 1D case. However, there are significant differences and complications because of the logarithmic singularity of the

https://doi.org/10.1017/S0956792511000015 Published online by Cambridge University Press

fundamental solution to the Laplacian in two dimensions. As a result, the scaling properties and stability range are very different from the 1D case.

As in one dimensions, we first construct the 2D steady state in the form of a hot spot, then study its stability. We first state the results for general domains; the location and stability of the spot involve the interaction of Green's function and the electric field strength $f(x)$. At the end of the section, we study in more detail the special case of a disk domain with radially symmetric $f(x) = f(|x|)$.

Principal Result 3.1 *Suppose that $d^2 p \gg 1$, with other parameters of $O(1)$. Consider the steady state equation in two dimensions,*

$$0 = \Delta u - \frac{1}{d^2} u + \alpha f(x) e^u, \quad x \in \Omega, \quad \partial_n u = 0, \quad x \in \partial\Omega, \tag{3.1}$$

$$\alpha := \frac{p e^u}{\left(d \int_\Omega f(x) e^u\right)^2}. \tag{3.2}$$

Then (2.1) admits a hot-spot solution. It is concentrated at the location x_0 given by

$$8\pi \nabla H_0 + \frac{\nabla f(x_0)}{f(x_0)} = 0, \tag{3.3}$$

where ∇H_0 is the gradient of the regular part of Green's function as defined by (3.16), (3.17), (3.20) and (3.24). The constant α, as defined in (3.2), is asymptotically given

$$\alpha \sim \frac{(8\pi d)^2}{p}. \tag{3.4}$$

Inside the hot spot, the temperature profile has the shape

$$u(x) \sim \ln\left\{\frac{8(1+R^2)^{-2}}{\alpha \mu^2 f(x_0)}\right\}, \quad R = |x - x_0|/\mu; \quad R = O(1),$$

where $\mu \ll 1$ is the spatial extent of the hot spot, asymptotically given by

$$\mu \sim 8\pi \exp(-2\gamma + 4\pi H_0) d^3 \sqrt{\frac{2 f_0}{p}}, \tag{3.5}$$

where $\gamma \approx 0.5772$ is Euler's constant. Away from the hot spot, the temperature profile has the shape

$$u \sim 8\pi G(x, x_0), \quad |x - x_0| \gg O(\mu), \tag{3.6}$$

where $G(x, x_0)$ is Green's function defined in (3.16).

We remark that a formula similar to (3.3) was obtained for the Liouville equation in [15] using a related technique. Next, we summarise the stability results.

Principal Result 3.2 *Let σ_1, σ_2 be the two eigenvalues of the matrix $8\pi M + F$, where M and F are defined in (3.48). Then the stability problem (3.33) admits two small eigenvalues*

https://doi.org/10.1017/S0956792511000015 Published online by Cambridge University Press

given by

$$\lambda \sim \frac{d^2}{2\ln \mu^{-1}}\sigma_i, \quad i = 1, 2.$$

All other eigenvalues are strictly negative.

Alternatively, let

$$g(x_0) = 4\pi H(x_0, x_0) + \ln f(x_0),$$

where H and f are as given in Principal Result 3.1. Then the location of the hot-spot solution satisfies $\nabla g(x_0) = 0$. Moreover, the hot spot is stable if x_0 is a non-degenerate maximum of $g(x_0)$, i.e. if the hessian of g at x_0 is definite negative. It is unstable if x_0 is either a non-degenerate saddle point or a non-degenerate minimum of g.

Derivation of Principal Result 3.1 As in one dimension, the derivation consists of two steps. We first derive the hot-spot profile, then determine its location.

Step 1. Hot-spot profile We expand near the inner region of the spike as

$$x = x_0 + \mu y, \tag{3.7}$$

$$f(x) = f_0 + \mu y f_0' + \cdots, \qquad \text{where } f_0 \equiv f(x_0), \quad f_0' \equiv \nabla f(x_0); \tag{3.8}$$

$$u(x) = U(y) = U_0(y) + \mu U_1(y) + \cdots, \tag{3.9}$$

where $\mu \ll 1$ is a scale parameter to be determined later. For convenience, we also let

$$U(y) = \ln\left\{\frac{V(y)}{\alpha\mu^2 f(x_0 + \mu y)}\right\} \tag{3.10}$$

and expand

$$V = V_0 + \mu V_1 + \cdots. \tag{3.11}$$

The equation for V_0 is then

$$\Delta_y V_0 - \frac{|\nabla_y V_0|^2}{V_0} + V_0^2 = 0. \tag{3.12}$$

A radial solution is given by

$$V_0(y) = \frac{8}{(1 + R^2)^2}, \quad R = |y|. \tag{3.13}$$

Note that (3.12) admits a scaling invariance $V_0 = a^{-2}\hat{V}_0; \quad y = a\hat{y}$. However, we can set $a = 1$ by an appropriate re-labelling of μ.

Next, we consider the outer region. Assuming $\alpha \ll 1$, we estimate

$$\Delta u - \frac{1}{d^2}u = -C_0\delta(x - x_0), \tag{3.14}$$

where δ is a delta function and the constant C_0 is given by

$$C_0 = \int_{-L}^{L} \alpha f(x) e^u dx \sim 2\pi \int_{-\infty}^{\infty} V_0(R) R dR \sim 8\pi. \tag{3.15}$$

https://doi.org/10.1017/S0956792511000015 Published online by Cambridge University Press

Now consider the modified Helmholtz G function that satisfies

$$\Delta G - \frac{1}{d^2} G = -\delta(x - x_0), \quad x \in \Omega; \qquad \partial_n G = 0, \quad x \in \partial\Omega. \tag{3.16}$$

Note that G has a logarithmic singularity as $x \to x_0$. In order to match the inner and outer solutions, decompose G as

$$G = J(x, x_0) + H(x, x_0), \quad r = |x - x_0|, \tag{3.17}$$

where J is Green's function on the entire space satisfying

$$\Delta J - \frac{1}{d^2} J = -\delta(x - x_0), \quad x, x_0 \in \mathbb{R}^2; \qquad J \to 0 \quad \text{as } |x| \to \infty, \tag{3.18}$$

and $H = G - J$ satisfies

$$\Delta H - \frac{1}{d^2} H = 0, \quad x \in \Omega; \qquad \partial_n H = -\partial_n J, \quad x \in \partial\Omega. \tag{3.19}$$

Explicitly, we have

$$J(x, x_0) = \frac{1}{2\pi} K_0\left(\frac{r}{d}\right), \qquad r = |x - x_0|, \tag{3.20}$$

where K_0 is the Bessel K function of order zero. In the outer region, we then obtain the solution to (3.14) for u is

$$u \sim 8\pi G(x, x_0), \quad |x - x_0| \gg O(\mu). \tag{3.21}$$

In order to match (3.21) to the inner solution (3.10), we expand

$$J \sim \frac{1}{2\pi} \ln \frac{1}{r} + \frac{1}{2\pi} (\ln(2d) - \gamma) + O(r^2 \ln r), \tag{3.22}$$

$$H \sim H_0 + (x - x_0) \cdot \nabla H_0, \tag{3.23}$$

where

$$H_0 = H(x_0, x_0); \ \nabla H_0 = \nabla H(x, x_0)|_{x = x_0}. \tag{3.24}$$

Writing the outer (3.21) solution in terms of the inner variables, we have

$$x - x_0 = \mu y; \quad R = |y|;$$

$$u \sim 4 \ln \frac{1}{\mu} + 4 \ln \frac{1}{R} + 4(\ln(2d) - \gamma) + 8\pi H_0 + \mu 8\pi y \cdot \nabla H_0 \ldots; \quad \mu \ll \mu R \ll 1. \tag{3.25}$$

Taking the limit $R \to \infty$ of the inner variables, we obtain

$$V_0 \sim \frac{8}{R^4}; \tag{3.26}$$

$$u \sim 4 \ln \frac{1}{R} + 2 \ln \frac{1}{\mu} + \ln\left(\frac{8}{\alpha f_0}\right). \tag{3.27}$$

https://doi.org/10.1017/S0956792511000015 Published online by Cambridge University Press

Equating (3.25) and (3.27) we get, for leading order,

$$4\ln\frac{1}{\mu}+4\left(\ln(2d)-\gamma\right)+8\pi H_0\sim 2\ln\frac{1}{\mu}+\ln\left(\frac{8}{\alpha f_0}\right),$$

$$\mu\sim\exp(-2\gamma+4\pi H_0)d^2\sqrt{2\alpha f_0}. \tag{3.28}$$

In order to determine the spatial extent of the spike in terms of p, we substitute (3.15) into (3.2) to obtain

$$\alpha\sim\frac{(8\pi d)^2}{p}. \tag{3.29}$$

Substituting (3.29) into (3.28) yields (3.5).

Step 2. Hot-spot location In order to determine the the hot-spot location, we consider the $O(\mu)$ correction terms to the steady state. From (3.11) and (3.9), we have

$$0=\Delta U_0+V_0, \tag{3.30}$$

$$0=\Delta U_1+V_0U_1+V_0y\cdot\frac{\nabla f_0}{f_0}. \tag{3.31}$$

In addition, we have

$$\Delta U_{0y_j}+V_{0y_j}=0;\quad V_{0y_j}=V_0U_{0y_j},$$

where $*_{y_j}$ denotes the derivative with respect to y_j, $j=1,2$. Let B be a ball of a large radius $R\to\infty$. Multiply (3.31) by U_{0j} and integrate over B. Integrating by parts we obtain

$$0=\int_{\partial B}(U_{0y_j}\partial_nU_1-\partial_nU_{0y_j}U_1)dS(y)+\int_B U_{0y_j}V_0y\cdot\frac{\nabla f_0}{f_0}dy,\quad j=1,2.$$

First consider the case $j=1$. In order to evaluate the boundary terms, note that the behaviour of U for large $|y|$ is obtained by taking the limit of the outer expansion for small x. From (3.25), we obtain

$$\begin{aligned}
&U_0\sim-4\ln R+O(1);\quad U_1\sim 8\pi R(\cos\theta,\sin\theta)\cdot\nabla H_0;\qquad R\to\infty\\
&U_{0y_1}\sim-\frac{4}{R}\cos\theta;\quad \partial_nU_{0y_1}\sim\frac{4}{R^2}\cos\theta;\\
&\partial_nU_1\sim 8\pi(\cos\theta,\sin\theta)\cdot\nabla H_0;
\end{aligned}$$

$$\begin{aligned}
\int_{\partial B}(U_{0y_1}\partial_nU_1-\partial_nU_{0y_1}U_1)dS(y)&\sim 2\int_0^{2\pi}-4\cos\theta 8\pi(\cos\theta,\sin\theta)\cdot\nabla H_0d\theta\\
&\sim-64\pi^2e_1\cdot\nabla H_0.
\end{aligned}$$

Finally, we have

$$\int_B U_{0y_1}V_0y\cdot\frac{\nabla f_0}{f_0}dy\sim\int_{\mathbb{R}^2}V_{0y_1}y\cdot\frac{\nabla f_0}{f_0}dy\sim-8\pi\frac{e_1\cdot\nabla f_0}{f_0}.$$

https://doi.org/10.1017/S0956792511000015 Published online by Cambridge University Press

Performing the same computation with $j = 2$, we finally obtain

$$8\pi\nabla H_0 + \frac{\nabla f_0}{f_0} = 0. \tag{3.32}$$

Stability in two dimensions. As in one dimension, we linearise

$$u(x,t) = u(x) + e^{\lambda t}\phi(x)$$

to obtain

$$\frac{\lambda}{d^2}\phi = \Delta\phi - \frac{1}{d^2}\phi + \alpha f(x)e^u\phi - 2\alpha^{3/2}p^{-1/2}d^{-1}f(x)e^u\int_\Omega f(x)e^u\phi\,dx. \tag{3.33}$$

First we consider the small eigenvalue corresponding to the translation invariance of the inner problem. In the inner region, the eigenfunction has the form

$$\phi = c_1\frac{V_{x_1}}{V} + c_2\frac{V_{x_2}}{V}, \tag{3.34}$$

$$\sim c_1u_{x_1} + c_2u_{x_2}. \tag{3.35}$$

The constants (c_1, c_2) indicate the direction of the instability. These will be determined at the same time as the eigenvalue. As in one dimension, the non-local term in (3.33) is of lower order due to the odd parity of the integrand

$$\int_\Omega fe^u\phi\,dx \sim \int_{\mathbb{R}^2}\frac{V}{\alpha\mu^2}\left(\frac{c_1V_{x_1} + c_2V_{x_2}}{V}\right)dx = 0.$$

There are now two solvability conditions to consider, corresponding to two undetermined constants c_1, c_2. Multiply (3.33) by u_{x_j}, $j = 1, 2$ and integrate by parts. We obtain

$$\frac{\lambda}{d^2}\int_\Omega \phi u_{x_j}dx \sim \int_{\partial\Omega}(u_{x_j}\partial_n\phi - \phi\partial_nu_{x_j})dS(x) + \int_\Omega\phi\left(\Delta u_{x_j} - \frac{1}{d^2}u_{x_j} + \alpha f(x)e^uu_{x_j}\right)dx.$$

Note that

$$\Delta u_{x_j} - \frac{1}{d^2}u_{x_j} + \alpha f(x)e^uu_{x_j} = -\alpha f_{x_j}e^u$$

so that

$$\frac{\lambda}{d^2}\int_\Omega\phi u_x dx \sim -\int_{\partial\Omega}\phi\partial_nu_{x_j}dS(x) - \int_\Omega\phi\alpha f_{x_j}e^u dx. \tag{3.36}$$

Now, away from the centre of the spike we have

$$\Delta\phi \sim \frac{1+\lambda}{d^2}\phi;\quad \Delta u_{x_j} \sim \frac{1}{d^2}u_{x_j},\quad x \neq x_0. \tag{3.37}$$

Now consider a domain $D = \Omega\backslash B_\delta(x_0)$, where $B_\delta(x_0)$ is a ball of small radius δ centred

https://doi.org/10.1017/S0956792511000015 Published online by Cambridge University Press

around x_0, with $\mu \ll \delta \ll 1$. We obtain

$$0 = \int_D \left(\Delta\phi - \frac{1+\lambda}{d^2}\phi\right) u_{x_j} dx = \int_{\partial\Omega\setminus B_\delta(x_0)} (u_{x_j}\partial_n\phi - \phi\partial_n u_{x_j}) dS(x) - \int_{\Omega\setminus B_\delta(x_0)} \frac{\lambda}{d^2}\phi u_{x_j} dx, \tag{3.38}$$

$$\int_{\partial\Omega} \phi\partial_n u_{x_j} dS(x) + \int_\Omega \frac{\lambda}{d^2}\phi u_{x_j} dx \sim \int_{B_\delta(x_0)} \frac{\lambda}{d^2}\phi u_{x_j} dx - \int_{\partial B_\delta(x_0)} (u_{x_j}\partial_n\phi - \phi\partial_n u_{x_j}) dS(x). \tag{3.39}$$

Substituting (3.39) into (3.36), we obtain

$$\int_{\partial B_\delta(x_0)} (u_{x_j}\partial_n\phi - \phi\partial_n u_{x_j}) dS(x) - \int_{B_\delta(x_0)} \frac{\lambda}{d^2}\phi u_{x_j} dx \sim \int_\Omega \phi\alpha f_{x_j} e^u dx. \tag{3.40}$$

Next, we evaluate the left-hand side. Recall that

$$u \sim -4\ln R, \quad R = |y| = |x-z|/\mu, \quad 1 \ll R \ll \frac{1}{\mu}$$

so that in the intermediate region, the leading-order behaviour is

$$\phi \sim c_1 u_{x_1} + c_2 u_{x_2} \sim \frac{-4}{r}(c_1\cos\theta + c_2\sin\theta); \quad \mu \ll r \ll 1, \tag{3.41}$$

where $r = |x-z|$. Therefore, ϕ solves (3.37) subject to singularity condition (3.41) as $r = |x-x_0| \to 0$. Now, let G^λ be Green's function satisfying

$$\Delta G^\lambda - \omega^2 G^\lambda = -\delta(x-z), \quad x \in \Omega; \qquad \partial_n G = 0, \quad x \in \partial\Omega; \qquad \omega^2 := \frac{1+\lambda}{d^2}. \tag{3.42}$$

Note that $G^\lambda(x,z) \sim -\frac{1}{2\pi}\ln r$ as $r \to 0$. It follows that $G^\lambda_{z_1} \sim \frac{1}{2\pi}\frac{\cos\theta}{r}$; $G^\lambda_{z_2} \sim \frac{1}{2\pi}\frac{\sin\theta}{r}$. By matching with (3.41), we obtain the following behaviour of ϕ in the outer region:

$$\phi \sim -8\pi\left(c_1 G^\lambda_{z_1} + c_2 G^\lambda_{z_2}\right), \quad r = O(1).$$

https://doi.org/10.1017/S0956792511000015 Published online by Cambridge University Press

Next we decompose G^λ into singular and regular part as in (3.17). We will need to keep terms up to $O(r^2)$. For reference, note that

$$K_0(r) \sim -\ln r + a_0 + \frac{r^2}{4}(-\ln r + a_0) + O(r^4 \ln r); \quad r \to 0, \quad \text{with} \quad a_0 = \ln 2 - \gamma,$$

where K_0 is the Bessel K function so that

$$G^\lambda \sim \frac{1}{2\pi}\left(-\ln r + a_0 - \ln \omega - \frac{\omega^2}{4} r^2 \ln r + O(r^2)\right) + H^\lambda(x,z) \quad \text{as} \quad z \to x, \quad \omega = \sqrt{\frac{1+\lambda}{d^2}};$$
$$r = |x - z|,$$

where $H^\lambda(x,z)$ is a C^2 function given by (3.19) with $\frac{1}{d^2}$ replaced by $\omega^2 = \frac{1+\lambda}{d^2}$. In the intermediate region, we then obtain

$$\phi \sim -8\pi \begin{pmatrix} -\left(c_1 \dfrac{\cos\theta}{2\pi} + c_2 \dfrac{\sin\theta}{2\pi}\right) g(r,\omega) \\ +c_1 H^\lambda_{z_1} + c_2 H^\lambda_{z_2} \end{pmatrix}, \quad \mu \ll r \ll 1,$$

where

$$g(r,\omega) = -\frac{1}{r} + \frac{\omega^2}{4}\left(2r\left(-\ln r + a_0 - \ln \omega\right) - r\right).$$

Similarly, for $\mu \ll r \ll 1$, we have

$$u_{x_1} \sim 8\pi\left[\frac{\cos\theta}{2\pi} g(r,\omega_0) + H_{x_1}\right], \quad \omega_0 = \frac{1}{d};$$
$$u_{x_2} \sim 8\pi\left[\frac{\sin\theta}{2\pi} g(r,\omega_0) + H_{x_2}\right].$$

Next, we compute

$$\partial_n \phi \sim -8\pi \begin{pmatrix} c_1\left(H^\lambda_{z_1 x_1}\cos\theta + H^\lambda_{z_1 x_2}\sin\theta\right) + c_2\left(H^\lambda_{z_2 x_1}\cos\theta + H^\lambda_{z_2 x_2}\sin\theta\right) \\ -\left(c_1 \dfrac{\cos\theta}{2\pi} + c_2 \dfrac{\sin\theta}{2\pi}\right) g_r(r,\omega) \end{pmatrix},$$

$$\partial_n u_{x_1} \sim 8\pi\left[\frac{\cos\theta}{2\pi} g_r(r,\omega_0) + \left(H_{x_1 x_1}\cos\theta + H_{x_1 x_2}\sin\theta\right)\right],$$
$$\partial_n u_{x_2} \sim 8\pi\left[\frac{\sin\theta}{2\pi} g_r(r,\omega_0) + \left(H_{x_2 x_1}\cos\theta + H_{x_2 x_2}\sin\theta\right)\right].$$

Now, note that

$$g(r,w) \sim -\frac{1}{r} - \frac{\omega^2}{2} r \ln r + O(r),$$
$$g_r(r,w) = \frac{1}{r^2} - \frac{\omega^2}{2}\ln r + O(1).$$

https://doi.org/10.1017/S0956792511000015 Published online by Cambridge University Press

It will be evident later on that $\lambda = O(1/\ln \mu^{-1}) \ll 1$. Therefore we have $\omega^2 - \omega_0^2 \sim \frac{\lambda}{d^2}$;

$$g(r,\omega_0)g_r(r,\omega) - g(r,\omega)g_r(r,\omega_0) \sim \frac{1}{r}\left[\frac{\lambda}{d^2}\ln r + O(\lambda) + O(r)\right], \quad \lambda, r \to 0.$$

Keeping in mind that λ is small, we then obtain

$$\int_{\partial B_\delta(x_0)} (u_{x_1}\partial_n\phi - \phi\partial_n u_{x_1})dx \sim (8\pi)^2(c_1(H_{z_1x_1} + H_{x_1x_1}) + c_2(H_{z_2x_1} + H_{x_2x_1})) + 16\pi c_1\frac{\lambda}{d^2}\ln\delta, \tag{3.43}$$

$$\int_{\partial B_\delta(x_0)} (u_{x_2}\partial_n\phi - \phi\partial_n u_{x2})dx \sim (8\pi)^2(c_1(H_{z_1x_2} + H_{x_2x_1}) + c_2(H_{z_2x_2} + H_{x_2x_2})) + 16\pi c_2\frac{\lambda}{d^2}\ln\delta. \tag{3.44}$$

Next, we evaluate $\int_{B_\delta(x_0)} \frac{\lambda}{d^2}\phi u_{x_j}dx$. The dominant contribution for this integral comes from the inner region. Therefore, using (3.13) we obtain

$$\begin{aligned}\frac{\lambda}{d^2}\int_{B_\delta(x_0)} \phi u_{x_j}dx &\sim \frac{\lambda}{d^2}\int_{B_{\delta/\mu}(0)} c_j U_{y_j}^2 dy \sim c_j\pi\frac{\lambda}{d^2}\int_0^{\delta/\mu}\left(\frac{-4R}{1+R^2}\right)^2 RdR \\ &\sim 16\pi c_j\frac{\lambda}{d^2}(\ln\delta - \ln\mu) + O(1).\end{aligned} \tag{3.45}$$

Note that the $\ln\delta$ term in (3.45) cancels precisely with the $\ln\delta$ term in (3.43) and (3.44) so that the left-hand side of (3.40) is indeed independent of δ. Next we evaluate $\int_\Omega \phi\alpha f_{x_j}e^u dx$. Using (3.10) and (3.34), we obtain

$$\begin{aligned}\int_\Omega \phi\alpha e^u f_{x_j}dx &\sim \frac{1}{\mu^2}\int_\Omega \sum_{i=1}^2 c_i (V)_{x_i}\left(\frac{f_{x_j}}{f}\right)dx, \\ &\sim -\frac{1}{\mu^2}\int_\Omega \sum_{i=1}^2 c_i\left(\frac{f_{x_j}}{f}\right)_{x_i} V dx \\ &\sim -8\pi\sum_{i=1}^2 c_i\left(\frac{f_{x_j}}{f}\right)_{x_i}\Bigg|_{x=x_0}.\end{aligned} \tag{3.46}$$

Substituting (3.43), (3.44), (3.45) and (3.46) into (3.40), we obtain the following equation for λ :

$$(8\pi M + F)\begin{pmatrix}c_1\\c_2\end{pmatrix} = \lambda\left(\frac{2}{d^2}\ln\mu^{-1}\right)\begin{pmatrix}c_1\\c_2\end{pmatrix}, \tag{3.47}$$

where

$$M = \begin{bmatrix}H_{z_1x_1} + H_{x_1x_1} & H_{z_2x_1} + H_{x_2x_1}\\ H_{z_1x_2} + H_{x_2x_1} & +H_{z_2x_2} + H_{x_2x_2}\end{bmatrix}\Bigg|_{x=x_0}; \quad F = \begin{bmatrix}\left(\frac{f_{x_1}}{f}\right)_{x_1} & \left(\frac{f_{x_1}}{f}\right)_{x2}\\ \left(\frac{f_{x_2}}{f}\right)_{x_1} & \left(\frac{f_{x_2}}{f}\right)_{x2}\end{bmatrix}\Bigg|_{x=x_0}. \tag{3.48}$$

https://doi.org/10.1017/S0956792511000015 Published online by Cambridge University Press

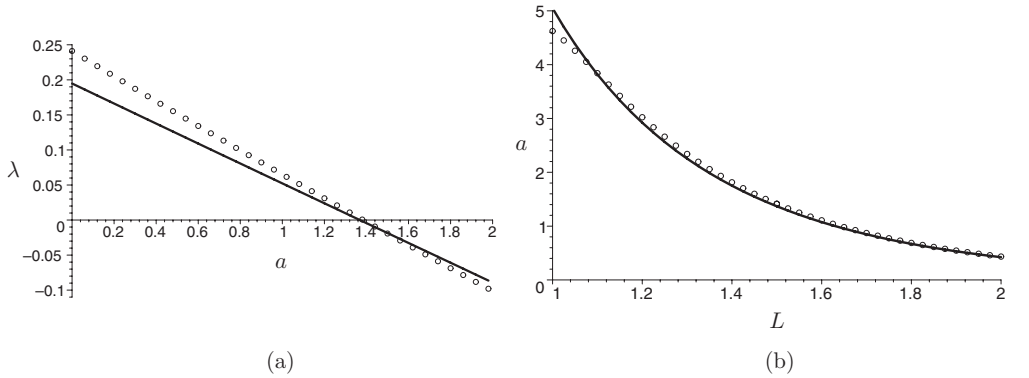

FIGURE 3. Comparison of numeric and asymptotic computations of the small eigenvalue λ for a 2D disk domain of radius L. (a) The graph of λ versus a, where $f(x) = \exp(-a|x|^2/2)$ and other parameters are $\alpha = 0.00125$, $L = 1.5$, $d = 1$. The solid curve is the asymptotic approximation given by (3.50). The dots are obtained by numerically solving the eigenvalue problem (3.33) using boundary value problem solver. (b) The threshold of stability $\lambda = 0$ in two dimensions with $d = 1$, $f(x) = \exp(-a|x|^2/2)$ and $\alpha = 0.005$. The solid curve is the asymptotic threshold given by $a = 2K_0''(L)/I_0''(L) - 2K_0'(L)/I_0'(L)$. The dotted points are obtained by numerically solving the eigenvalue problem (3.33) for $\lambda = \lambda(a)$, then using a root finder to solve for $\lambda = 0$. The hot spot is unstable for parameter values below the curve and is stable for parameter values above the curve.

In particular, assuming that matrix $4\pi M + F$ is $O(1)$, it follows that $\lambda = O(d^2/\ln(\mu^{-1})) \ll 1$, since $\mu \ll 1$. Note that there are in general two small eigenvalues, corresponding to the two eigenvalues of the matrix $4\pi M + F$. This concludes the derivation.

Disk domain. Next, specialise the results of Principal Result 3.2 to a disk of radius L, with a radially symmetric electric field strength $f(x) = f(|x|)$. The goal is to derive the explicit instability threshold given in (1.4). We assume that the hot spot is radially symmetric and located at the centre of the disk. In this case, the expressions in (3.48) can be significantly simplified as follows. First, note that when $z = 0$, the solution G to (3.16) can be explicitly written as

$$G(x,z)|_{z=0} = \frac{1}{2\pi}\left(K_0(\omega r) - \frac{K_0'(\omega L)}{I_0'(\omega L)} I_0(\omega r)\right), \quad r = |x|\,; \quad \omega = \frac{1}{d},$$

$$H(x,z)|_{z=0} = -\frac{1}{2\pi}\left(\frac{K_0'(\omega L)}{I_0'(\omega L)}\right).$$

On the other hand, let $v(x) = G_{z_1}(x,z)|_{z=0}$. Now, we have $2\pi G \sim -\ln(|x-z|)$ as $x \to z$ so that $2\pi G_{z_1}|_{z=0} \sim \frac{\cos\theta}{r}$, $r = |x| \to 0$. It follows that v solves

$$\begin{aligned} \Delta v - \omega^2 v &= 0, \quad x \in B_L(0), \\ v &\sim \frac{\cos\theta}{2\pi r}, \quad r = |x| \to 0, \\ \partial_n v &= 0, \quad r = L. \end{aligned}$$

Thus, we obtain that $v(x) = (\cos\theta)J(r)$, where $J(r)$ solves the Ordinary Differential

https://doi.org/10.1017/S0956792511000015 Published online by Cambridge University Press

Equation

$$J_{rr} + \frac{1}{r}J_r - \frac{1}{r^2}J - \omega^2 J = 0, \tag{3.49}$$

subject to boundary conditions

$$J'(L) = 0; \quad J(r) \sim \frac{1}{2\pi r} \quad \text{as } r \to 0.$$

The particular solutions to (3.49) are given by $K_0'(r\omega)$, $I_0'(r\omega)$, with $K_0'(r\omega) \sim \frac{-1}{\omega r}$ so that we get

$$J(r) = -\frac{\omega}{2\pi}\left(K_0'(r\omega) - \frac{K_0''(\omega L)}{I_0''(\omega L)} I_0'(r\omega)\right).$$

Therefore we obtain

$$H_{x_1} = -\frac{\omega}{2\pi}\frac{K_0'(\omega L)}{I_0'(\omega L)}\left(I_0'(\omega r)\right)(\cos\theta),$$
$$H_{z_1} = \frac{\omega}{2\pi}\frac{K_0''(\omega L)}{I_0''(\omega L)}\left(I_0'(r\omega)\right)(\cos\theta).$$

We further compute

$$\begin{aligned}(H_{x_1x_1})_{r=0} &= \left((H_{x_1})_r \cos\theta - \frac{1}{r}(H_{x_1})_\theta \sin\theta\right)_{r=0} \\ &= -\frac{\omega}{2\pi}\frac{K_0'(\omega L)}{I_0'(\omega L)}\left(\omega I_0''(\omega r)\cos^2\theta + \frac{1}{r}I_0'(\omega r)\sin^2\theta\right)_{r=0} \\ &= -\frac{\omega^2}{4\pi}\frac{K_0'(\omega L)}{I_0'(\omega L)}\end{aligned}$$

(where we have used the Taylor series expansion $I_0(t) \sim 1 + t^2/4$, $t \to 0$) and in the same way,

$$(H_{z_1x_1})_{r=0} = \frac{\omega^2}{4\pi}\frac{K_0''(\omega L)}{I_0''(\omega L)}.$$

Similarly,

$$\begin{aligned}(H_{z_1x_1})_{r=0} &= \left((H_{z_1})_r \sin\theta + \frac{1}{r}(H_{z_1})_\theta \cos\theta\right)_{r=0} \\ &= 0; \\ (H_{z_1x_1})_{r=0} &= 0\end{aligned}$$

so that

$$H_{z_1x_1} + H_{x_1x_1} = \frac{\omega_0^2}{4\pi}\left(\frac{K_0''(\omega_0 L)}{I_0''(\omega_0 L)} - \frac{K_0'(\omega_0 L)}{I_0'(\omega_0 L)}\right).$$

https://doi.org/10.1017/S0956792511000015 Published online by Cambridge University Press

The expressions involving z_2 in (3.48) are evaluated in the same way. Finally, for a radially symmetric function $f(x) = f(r)$ we obtain

$$\left[\left(\frac{f_{x_1}}{f}\right)_{x_1}\right]_{x=0} = \left[\left(\frac{f_{x_2}}{f}\right)_{x_2}\right]_{x=0} = \left(\frac{f'(r)}{f(r)}\right)'_{r=0} = \frac{f''(0)}{f(0)};$$
$$\left[\left(\frac{f_{x_2}}{f}\right)_{x_1}\right]_{x=0} = \left[\left(\frac{f_{x_2}}{f}\right)_{x_1}\right]_{x=0} = 0.$$

Thus, we obtain

$$\lambda \sim \frac{1}{\ln \mu^{-1}} \left\{ \left(\frac{K_0''(L/d)}{I_0''(L/d)} - \frac{K_0'(L/d)}{I_0'(L/d)} \right) + \frac{d^2}{2} \frac{f''(0)}{f(0)} \right\}. \tag{3.50}$$

Figure 3 shows a favorable comparison between the asymptotic formula (3.50) and the numerical solution (3.33).

Using the Van-Dyke matching, we obtain the following simple uniform solution on a disk of radius L:

$$u_{\text{unif}} \sim 4 \left(K_0(r/d) - \frac{K_0'(L/d)}{I_0'(L/d)} I_0(r/d) \right) - 2\ln(1 + (r/\mu)^2), \tag{3.51}$$

where μ is given by Principal Result 3.1.

4 Large eigenvalues, single spot

In order to conclude the stability analysis of a single hot spot, we now prove the stability with respect to the large eigenvalues in one and two dimensions. The proof for one dimension has appeared elsewhere (see, for example, [11] or [4]). We include it here for completeness. Here, we follow [11]. In two dimensions, the situation is slightly more complicated because of the presence of a scaling invariance, which yields an extra zero eigenvalue.

We start by studying the local operator

$$L_0 \Phi = \Delta \Phi + V_0 \Phi, \tag{4.1}$$

where V_0 is given by (2.13) in one dimension or (3.12) in two dimensions. We have the following characterisation of the non-negative spectrum of (4.1).

Lemma 4.1 *Consider the local eigenvalue problem on all of* $\mathbb{R}^n$,

$$L_0 \Phi = \Lambda \Phi; \quad |\Phi(y)| \text{ is bounded as } |y| \to \infty. \tag{4.2}$$

with $n = 1$ *or* $n = 2$. *It admits a single strictly positive eigenvalue* $\Lambda = \Lambda_0 > 0$ *corresponding to a positive eigenfunction. In* $\mathbb{R}^1$, *(4.2) admits one zero eigenvalue; the corresponding eigenfunction is due to translation invariance and is given by*

$$Z_1 = \left(\frac{\partial}{\partial y} V_0(y) \right) / V_0.$$

https://doi.org/10.1017/S0956792511000015 Published online by Cambridge University Press

In $\mathbb{R}^2$*, (4.2) admits three zero eigenvalues given by*

$$Z_1 = \cos\theta \left(\frac{\partial}{\partial R} V_0\right)/V_0, \quad Z_2 = \sin\theta \left(\frac{\partial}{\partial R} V_0\right)/V_0, \quad Z_3 = 2 + R\left(\frac{\partial}{\partial R} V_0\right)/V_0, \quad (4.3)$$

where $R = |y|$*. The first two are due to translation invariance and the third is due to the scaling invariance. All other eigenvalues are strictly negative.*

Proof We first note that Z_3 satisfies $L_0\Phi = 0$ in both one and two dimensions. In order to see this, let $U = \ln(V_0)$ so that U satisfies

$$\Delta U + e^U = 0. \quad (4.4)$$

This equation has a symmetry: If we write $U(R) = w(e^{\beta/2}R) + \beta$ then $w(z)$ also satisfies (4.4). Therefore, differentiating (4.4) with respect to β and then setting $\beta = 0$, we obtain that $Z_3 = \partial U/\partial\beta$ satisfies $L_0\Phi = 0$. In the same way, it is also easy to see that Z_1 and Z_2 correspond to translational invariance of (4.4). Now in one dimension, note that $Z_3 \sim O(R)$ for large R, so it is not bounded at infinity. On the other hand, in two dimensions, we have $Z_3 = O(1)$ for large R, so Z_3 satisfies (4.2) in two dimensions but not in one dimension.

Next, note that Z_1 has one root in one dimension. Therefore, by oscillation theorem, there must be an eigenfunction that has no roots, and whose eigenvalue is positive. Moreover, such an eigenfunction is unique, again by oscillation theorem. Similarly, in two dimensions, the eigenfunctions corresponding to the zero eigenvalue, Z_1, Z_2, Z_3 all have a single nodal line, which implies the existence of a unique strictly positive eigenvalue. It remains to prove that there are no other zero eigenvalues. In one dimension, this is true because the second order ODE $L_0\Phi = 0$ has only two solutions (Z_1 and Z_3) so by uniqueness of solution of an ODE, no other zero eigenfunctions can exist. In two dimensions, we decompose in polar coordinates, $\Phi(r,\theta) = \Phi(r)(A\cos m\theta + B\sin m\theta)$, where m is an integer. When $m = 0$ or $m = 1$, there are exactly three solutions to $L_0\Phi = 0$, given by Z_1, Z_2, Z_3, each having one nodal line. If $m > 1$, then Φ has at least two nodal lines, which correspond to roots of $A\cos m\theta + B\sin m\theta = 0$. But this implies that the corresponding eigenvalue $\lambda < 0$ by the Oscillation theorem (see for example [17], exercise 10 in Section 11.6). □

Remark 1 Note that the *inner* eigenvalue problem (4.2) is somewhat non-standard, as there is no linear decay-type term on the right-hand side. As such, it has a continuous spectrum up to $\mathrm{Re}(\Lambda) \leqslant 0$. However, the *outer* problem (2.9) or (3.33) does have a decay since the outer region away from the spike is of the form $\lambda\phi \sim d^2\Delta\phi - \phi$. Therefore, any continuous spectrum must satisfy $\mathrm{Re}(\lambda) \leqslant -1$. As such, the presence of continuous spectrum does not affect the stability of the hot spot.

Remark 2 In one dimension, the unique positive eigenvalue of (4.2) is $\Lambda_0 = 1/4$; the corresponding eigenfunction is $\mathrm{sech}(y/2)$ (see [11]). In two dimensions, we do not know an explicit formula, but numerically we obtain $\Lambda_0 \approx 2.545$.

https://doi.org/10.1017/S0956792511000015 Published online by Cambridge University Press

Next, consider the non-local problem

$$L_0\Phi - \gamma V_0 \int_{\mathbb{R}^n} V_0 \Phi dy = \Lambda\Phi; \quad \Phi(y) \to 0 \quad \text{as } |y| \to \infty. \tag{4.5}$$

Note that $L_0 1 = V_0$ so that $\Phi = 1$ is an eigenfunction of (4.5) corresponding to the zero eigenvalue whenever $\gamma = \gamma_0$, where

$$\gamma_0 = \frac{1}{\int_{\mathbb{R}^n} V_0 dy}. \tag{4.6}$$

Next, we show the following.

Principal Result 4.1 *Consider the non-local eigenvalue problem (4.5). Suppose that $\gamma > \gamma_0$. Then, the problem (4.5) has no strictly positive eigenvalues. The zero eigenspace is the same as that of a local problem (4.2) and is given in Lemma 4.1. On the other hand, if $\gamma < \gamma_0$ then there is a strictly positive eigenvalue of (4.5).*

Proof Given an eigenfunction Φ of (4.5), there are two cases to consider. Either $\int V_0\Phi$ is zero or not. In the former case, by Lemma 4.1, $\Lambda \leqslant 0$. In the latter case, by scaling Φ appropriately, (4.5) becomes

$$\gamma V_0 = (L_0 - \Lambda)\Phi; \qquad \int_{\mathbb{R}^n} V_0 \Phi dy = 1.$$

Define

$$f(\Lambda) = \int_{\mathbb{R}^n} V_0 (L_0 - \Lambda)^{-1} V_0 dy$$

so that Λ corresponds to the solution of $f(\Lambda) = 1/\gamma$. We now study the graph of $f(\Lambda)$. Using integration by parts, we have

$$f'(\Lambda) = \int_{\mathbb{R}^n} ((L_0 - \Lambda)^{-1} V_0)^2 dy > 0.$$

Also, note that $f(0) = 1/\gamma$ and $f \to 0$ as $\Lambda \to \infty$. Moreover, $f(\Lambda)$ has a vertical asymptote near $\Lambda = \Lambda_0$, the positive eigenvalue of the local operator L_0. Since Λ_0 is the only strictly positive eigenvalue of L_0, $f(\Lambda)$ has no other singularities for $\Lambda > 0$. This shows that $f(\Lambda) > \frac{1}{\gamma}$ on $(0, \Lambda_0)$ and $f(\Lambda) < 0$ on (Λ_0, ∞). So, if $\gamma > \gamma_0$ then there are no solutions to $f(\Lambda) = \frac{1}{\gamma}$; on the other hand, there is a solution $\Lambda \in (0, \Lambda_0)$ to $f(\Lambda) = \frac{1}{\gamma}$ if $\gamma < \gamma_0$.

Finally, it is easy to verify that $\int_{\mathbb{R}^n} V_0 Z_i dy = 0$ for $i = 1$ (in $\mathbb{R}^1$) or $i = 1, 2, 3$ (in $\mathbb{R}^2$). This shows that the null space of L_0 is also in the zero eigenspace of (4.5). On other hand, if Φ an eigenfunction corresponding to a zero eigenvalue, then either $\int_{\mathbb{R}^n} V_0 \Phi dy = 0$ – in which case Φ is a linear combination of Z_i – or else by choosing an appropriate re-scaling we have

$$L_0\Phi = V_0, \quad \gamma \int_{\mathbb{R}^n} V_0 \Phi dy = 1.$$

But then $\Phi = 1$ and $\gamma = \gamma_0$. This completes the proof. □

https://doi.org/10.1017/S0956792511000015 Published online by Cambridge University Press

Principal Result 4.1 shows that the stability of the full problem (2.9) or (3.33) depends only on the stability of the small eigenvalues whose eigenfunctions in the inner region correspond to the kernel of L_0 as given in Lemma 4.1. Now in one dimension, this kernel consists of translational mode Z_1, whose instability was classified in Principal Result 2.2. In two dimensions, the kernel consists of two translation modes Z_1, Z_2, which were classified in Principal Result 3.2, and of a scaling eigenfunction Z_3. Now we note that $Z_3 \sim$ constant as $R = |x - x_0|/\mu \to \infty$. On the other hand, in the outer region we have

$$d^2 \Delta \phi - \phi \sim \lambda \phi, \quad |x - x_0| \gg O(\mu),$$

with Neumann condition at the boundaries. In order to match with the inner region, ϕ must be bounded as $|x - x_0| \to 0$. But then we must have $\lambda \sim -1$, since $\phi \not\equiv 0$. This shows that the eigenvalue corresponding to the scaling mode Z_3 is stable.

5 Non-singular solutions; two hot spots

For some values of p, it is possible to construct non-singular perturbation solutions. For leading order, such solutions satisfy the differential equation (1.3) with d set to 0. In this case, the leading-order behaviour of the solution must satisfy the implicit relation

$$u = d^2 \alpha f(x) e^u. \tag{5.1}$$

In order to determine the critical value of p when such solutions exist, we consider the relation $u = \beta e^u$. This relation will have no solutions for $\beta > \frac{1}{e}$, one solution for $\beta = \frac{1}{e}$ and two solutions otherwise. Thus, to find the critical value of p, we solve for $u = \frac{f(x)}{M} e^{u-1}$, where $M = \max_\Omega |f(x)|$. We may then evaluate α as

$$\alpha = \frac{p}{\left(d \int_\Omega MeW\left(-\frac{f(x)}{Me}\right) dx \right)^2},$$

where $W(x)$ is the principle branch of the Lambert W function. At the critical value of p, $\alpha = \frac{1}{d^2 Me}$. We can then solve for the critical value of p as

$$p_c = Me \left(\int_\Omega W\left(-\frac{f(x)}{Me}\right) dx \right)^2. \tag{5.2}$$

For $p < p_c$, there will be two non-singular perturbation solutions. As for the leading order, the partial differential equation is reduced to an ordinary differential equation at each point x, it is evident that the smaller solution is stable and the larger unstable.

In order to illustrate the existence of such solutions, consider the 2D unit disk with

$$f(x) = \cos(\theta)^2 \, \mathrm{J}_1(z_1 r)^2, \tag{5.3}$$

where z_1 is the first root of $\mathrm{J}_1(z)$ the Bessel function of the first kind of order 1. Such an electric field results from using a TM_{111} wave guide with the wafer placed near the bottom of the cavity on pegs [14]. Using (5.3), we then compute from (5.2) that $p_c \sim 1.35$. Next, we take $p = 1.3$. Solving (5.1), we then obtain Figure 4(a). On the other hand, we

https://doi.org/10.1017/S0956792511000015 Published online by Cambridge University Press

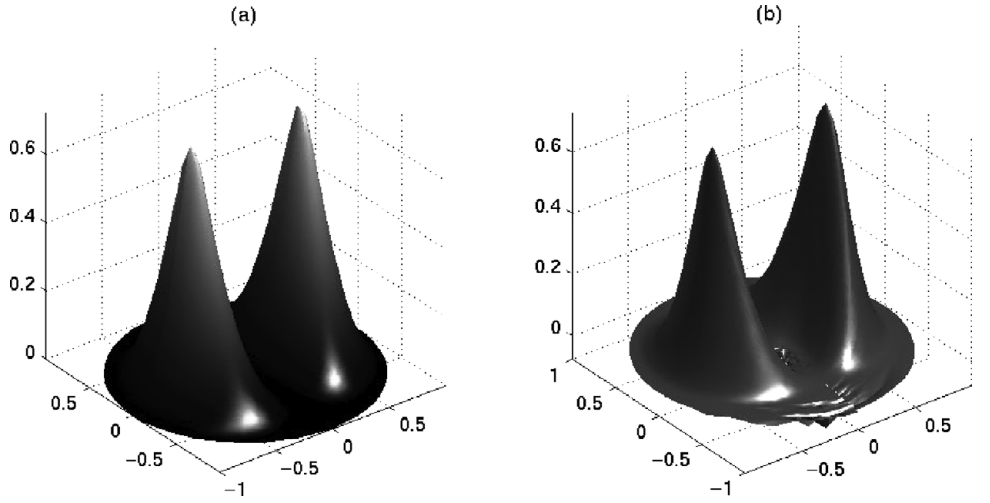

FIGURE 4. Comparison of solution to (5.1) and the full numerical simulation of (1.3) on a unit disk. The electric field $f(x)$ is taken to be (5.3), $p = 1.3$ and $d = 0.05$. (a) Solution given by (5.1). (b) Full numerical simulation of (1.3) using FlexPDE. Initial conditions were taken to be a constant and the simulation quickly reached a steady state which is shown here.

used FlexPDE software [3] to simulate the full PDE (1.3). Using $d = 0.01$ and a constant initial condition $u(x, 0) = 0.1$, the solution quickly settles to a steady state, which is shown in Figure 4(b). It is seen to be in good agreement with the steady state given by (5.1).

If $p > p_c$, then the non-singular solutions will not exist. In order to illustrate this, we again consider $f(x)$ given by (5.3) but take $p = 1.4 > p_c = 1.35$. We also took $d = 0.01$ and the initial condition $u(x, 0) = 0.1$. The resulting solution is shown in Figure 5. Since p is close to p_c, numerical simulation shows that initially the solution resembles the non-singular solution of Figure 4. Such transient state then evolves into a solution that consists of two hot spots located near the maxima of $f(x)$. However, this two hot-spot solution itself is unstable; one of the spots is quickly destroyed. Finally, the resulting solution containing only one hot spot appears to settle to a stable equilibrium.

The instability of two-spot solutions can be seen as follows. As discussed in Section 4, the spectrum of the local problem (4.2) contains an $O(1)$ positive eigenvalue Λ_0 with a strictly positive eigenfunction Z_0. Now, consider $\phi = \frac{1}{f(x_0)} Z_0(\frac{|x-x_0|}{\epsilon}) - \frac{1}{f(x_1)} Z_0(\frac{|x-x_1|}{\epsilon})$. Due to the symmetry of the solution and the localised nature of Z_0, the integral term of the non-local eigenvalue problem (4.5) will vanish, reducing it to the local eigenvalue problem (4.2). It follows that $\lambda > 0$ is an eigenvalue of the two-spot configuration. This unstable eigenvalue is responsible for the competition-type instability observed in Figure 5.

6 Discussion

For a homogeneous electric field ($f(x) =$ constant), it was shown in [8] that the hot spot exhibits a metastable behaviour and slowly moves to the boundary of the domain [8]. On the other hand, for the case where the non-linearity in (1.1) is $G(u) = u^2$, it was also shown in [8] that in the limit of small diffusivity, the 1D hot spot will concentrate at the

https://doi.org/10.1017/S0956792511000015 Published online by Cambridge University Press

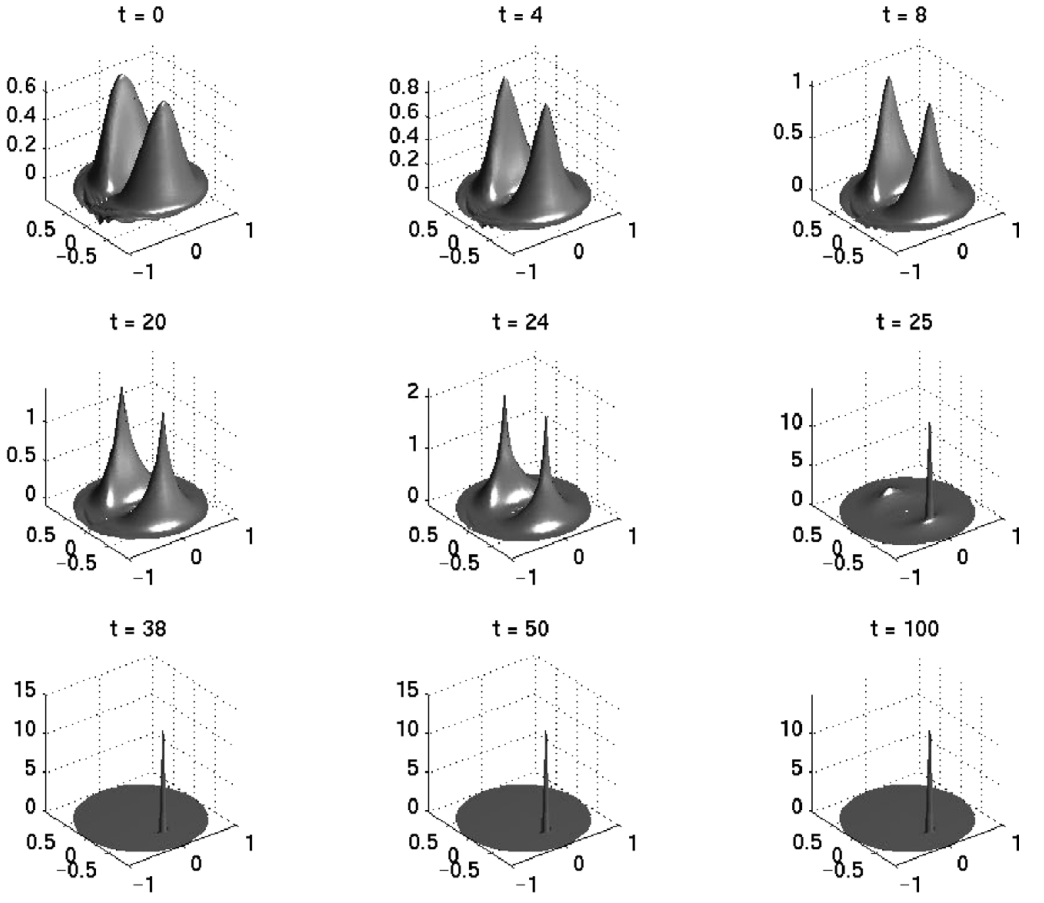

FIGURE 5. A simulation of (1.3) with $p = 0.14$. We use the f and initial conditions as in (4).

maximum of $f(x)$. This is more complicated when the non-linearity is exponential and the power p is sufficiently large. In such a case, the position of the hot spot is determined by a combination of $f(x)$, the power p and the domain geometry (see Principal Result 2.1). As Formula (1.6) shows, the hot spot can lose its instability in the 1D case even with $d \ll 1$, when p is increased sufficiently so that

$$p > d^2 \exp\left(\frac{|f''(0)|d^2}{4f(0)} \exp(2L/d)\right).$$

The 2D case is more difficult to analyse due to the appearance of the logarithmic singularity in the free-space Green's function. Unlike the 1D case, the stability is independent of the power p, and the hot spot will be stable provided that the diffusion $d \ll 1$ and $f(x)$ has an interior maximum. Moreover, 2D hot spot can be stable even when $d = O(1)$, provided that the relationship (1.4) holds. By contrast, the 1D hot spot is unstable when $d = O(1)$, regardless of the shape of $f(x)$.

https://doi.org/10.1017/S0956792511000015 Published online by Cambridge University Press

It is well known that scalar local reaction–diffusion systems cannot give rise to stable hot-spot-type solutions [2]. On the other hand, the addition of a non-local term has a stabilising effect [4, 6, 18]. Even then, two or more hot-spot solutions are found to be unstable – similar phenomenon was discussed in [7, 9] in the context of reaction–diffusion systems. It is an open question as to whether several hot-spot solutions can be stabilised.

The instability of the small eigenvalue typically induces a motion of the hot spot. In the case when d is small, the equations of motion of the spot in one dimension were derived in [8]; such motion was shown to be metastable (exponentially slow in d). Presumably, an extension to two dimensions should be along similar lines. However, when d is of $O(1)$, the expression for small eigenvalues is implicit in one dimension (see (2.42)). This complicates the derivation of the equations of motion of the spot.

Another open problem is to extend the modelling and analysis to the 3D case. For the exponential non-linearity, the inner problem leads to the Bratu equation

$$U_{rr} + \frac{2}{r}U + \lambda \exp(U) = 0, \quad U'(0) = 0.$$

The hot-spot solutions have the property that $U(0) \to \infty$ with $\lambda \to 2$ [10]. This makes it difficult to match the inner and outer solutions properly.

Finally, it would be interesting to study the stability and dynamics of a hot spot along the boundary; this is of interest, for example if $f(x)$ has no interior maximum, in which case the interior spot is unstable. Presumably, it will then move towards the boundary, and its eventual equilibrium location would depend on the balance between the magnitude of the electric field $f(x)$ and the geometry of the domain.

Acknowledgements

The authors are grateful to Prof. M. J. Ward for useful discussions and many suggestions, which helped to improve the presentation. A. Alcolado was supported by NSERC undergraduate summer research award. T. Kolokolnikov and D. Iron are supported in part by NSERC discovery grants. T. Kolokolnikov would like to thank Taida Institute for Mathematical Sciences, National Taiwan University for their hospitality and support during the writing of this paper.

References

[1] Booty, M. R. & Kriegsmann, G. A. (1994) Microwave heating and joining of ceramic cylinders: A mathematical model. *Methods Appl. Anal.* **1**(4), 403–414.

[2] Casten, R. & Holland, C. (1978) Instabifity results for reaction-diffusion equations with Neumann boundary conditions. *J. Differ. Equ.* 27, 266–273.

[3] FlexPDE software. Accessed 27 January 2011, see URL: www.pdesolutions.com.

[4] Freitas, P. (1994) Bifurcation and stability of stationary solutions of nonlocal scalar reaction-diffusion equations. *J. Dyn. Differ. Equ.* **6**(4), 613–629.

[5] Hill, J. M. & Marchant, T. R. (1996) Modelling microwave heating. *Appl. Math. Modelling*, **20**, 3–15.

[6] Iron, D. & Ward, M. (2000) A metastable spike solution for a nonlocal reaction-diffusion model. *SIAM J. Appl. Math.* **60**(3), 778–802.

https://doi.org/10.1017/S0956792511000015 Published online by Cambridge University Press

[7] Iron, D. & Ward, M. (2001) Spike pinning for the Gierer-Meinhardt model. *J. Math. Comput. Simul.* **55**, 419–431.
[8] Iron, D. & Ward, M. J. (2004) The stability and dynamics of hot-spot solutions for a one-dimensional microwave heating model. *Anal. Appl.* **2**(1), 21–70.
[9] Iron, D., Ward, M. J. & Wei, J. (2001) The stability of spike solutions to the one-dimensional Gierer-Meinhardt model. *Physica* D **150**, 25–62.
[10] Joseph, D. D. & Lundgren, T. S. (1973) Quasilinear Dirichlet problems driven by positive sources. *Arch. Ration. Mech. Anal.* **49**, 241–269.
[11] Kolokolnikov, T., Winter, M. & Wei, J. (2009) Existence and stability analysis of spiky solutions for the Gierer-Meinhardt system with large reaction rates. *Physica* D*: Nonlinear Phenom. Vol.* **238**(16), 1695–1710.
[12] Kriegsmann, G. A. (1997) Hot spot formation in microwave heated ceramic fibres. *IMA J. Appl. Math.* **59**(2), 123–148.
[13] Kriegsmann, G. A. (2001) Pattern formation in microwave heated ceramics: Cylinders and slabs. *IMA J. Appl. Math.* **66**(1), 1–32.
[14] Kriegsmann, G. A. (2005) *Microwave Heating of Materials: A Mathematical and Physical Overview*, distinguished colloquium given at Institute of Applied Mathematics, University of British Columbia.
[15] Ma, L. & Wei, J. (2001) Convergence for a Liouville equation. *Comment. Math. Helv.* **76**, 506–514.
[16] Roussy, G., Bennani, A. & Thiebiant, J. (1987) Temperature runaway of microwave irradiated materials. *J. Appl. Phys.* **62**, 1167–1170.
[17] Strauss, W. A. (1992) *Partial Differential Equations, an Introduction*, John Wiley & Sons, New York.
[18] Wei, J. (1999) On single interior spike solutions of the Gierer-Meinhardt system: Uniqueness and spectrum estimate. *Eur. J. Appl. Math.* **10**, 353–378.

https://doi.org/10.1017/S0956792511000015 Published online by Cambridge University Press